Article DOI: 10.1144/jgs2016-066

Article number: jgs2016-066

Article-type: research-article

Subject: Research article

Author please note

Proofs should not be posted to any website or server. You can post your accepted manuscript 12 months after publication.

Please check this proof carefully for errors, once it is published online no further changes can be made. In particular check that figures, tables and equations are correct.

This is an Online First paper. Until issue publication and page numbers are confirmed, please cite this article as: Kjetil Indrevær, Roy H. Gabrielsen and Jan Inge Faleide [year]. Early Cretaceous synrift uplift and tectonic inversion in the Loppa High area, southwestern Barents Sea, Norwegian shelf. *Journal of the Geological Society,* first published online [month] [date], [year], http://dx.doi.org/10.1144/jgs2016-066 (where square bracketed text should be updated with actual dates).

Author queries (see AQ? in margins)

No	Query
1	Please check this proof carefully for errors; once it is published online no further changes can be made. In particular, please check that figures are correct.
2	In sentence ‘It overlies a …’ should Faleide *et al*. 1993 be 1993*a* or 1993*b*,’ or both?
3	In sentence ‘Erosion of the high …’ please confirm change to ‘to the same level as the wider’ is OK.
4	In sentence ‘The Hammerfest Basin …’ please confirm change to ‘that have resulted in’ is OK.
5	In sentence ‘The concentric shape …’ should text be changed to ‘of the depocentre controlled’?
6	In sentence ‘The anticline encompasses …’ - Mulrooney *et al.* in preparation - if this reference can be updated (i.e. at least ‘in press’) please add publication details to reference list and amend both text citations.
7	In sentence ‘Numerical modelling has …’ Cloething & Burov 2011 - please provide full publication details or delete the citation. Also, please check spelling ‘Cloething’
8	Berglund *et al*. 1986 - please add book editor/s.
9	Doré 1991 is not cited in the text. Please cite or delete it.
10	Faleide *et al*. 1984 - please add page numbers of paper.
11	Faleide *et al*. 2015 - please give book editor/s, publisher’s name + city, and page number of abstract (or the abstract number).
12	Gabrielsen *et al*. 1993 - please give book editor/s.
13	Gabrielsen *et al*. 2005 - please add book editor/s and title of Special Publication.
14	Gabrielsen *et al*. 2011 - please add page number/s of abstract or abstract number.
15	Glørstad-Clark et al. 2011 - please clarify: how can a multi-author paper be part of a single-author thesis? Please amend this reference as necessary (use just the Glørstad-Clark thesis as the reference?)
16	Riis et al. 1986 - please add publication details.
17	Ritzmann & Faleide 2007 - please add page numbers of paper or doi.
18	Rønnevik *et al*. 1982 - please add book editor/s.
19	Stewart *et al*. 1995 - please add book editor/s, and title of Special Publication.
20	Wood *et al*. 1989 - please add book editor/s.
21	Fig. 5 - should location of part (c) be indicated in (a)?
22	Fig. 7 caption - should ‘see Fig. 3’ be changed to ‘see Fig. 2’?

Research article
JGS
Journal of the Geological Society
Published Online First
doi:10.1144/jgs2016-066

Early Cretaceous synrift uplift and tectonic inversion in the Loppa High area, southwestern Barents Sea, Norwegian shelf

Kjetil Indrevær*, **Roy H. Gabrielsen & Jan Inge Faleide**

Research Centre for Arctic Petroleum Exploration (ARCEx), Department of Geosciences, University of Oslo, Sem Sælands vei 1, 0371 Oslo, Norway

* Correspondence: kjetil.indrevar@geo.uio.no

Abstract: Tectonic inversion of rift basins is most commonly reported in the literature to occur after rifting has ceased. In contrast, we present evidence for synrift, localized tectonic inversion from the Loppa High area, southwestern Barents Sea and present a model for the formation of inversion structures as a result of differential uplift. The structures are of early Barremian to mid-Albian age (*c.* 131 – 105 Ma) and are focused in or near pre-existing extensional boundary faults along the margins of the Loppa High. Inversion is interpreted to be the result of uplift of the high along its inclined boundary faults, leading to space accommodation problems as uplift was not properly compensated by extension in the region. The model constrains the initiation of uplift of the Loppa High to the early Barremian and shows that the asymmetric margin configuration of the high may have led to a bulk clockwise rotation of the high around a vertical axis during uplift. The cause of uplift is not fully understood, but is suggested to be linked to contemporaneous extreme lithospheric thinning in neighbouring basins to the west. Processes involved may include isostatic flexure, thermal heating, lithological phase changes and/or far-field stresses, although these aspects need to be further tested.

Received 6 June 2016; **revised** 2 September 2016; **accepted** 7 September 2016

The present-day Barents Sea forms an epicontinental sea located in the northwestern corner of the Eurasian tectonic plate. It overlies a tectonically extended shelf that is composed of a range of basins, highs and fault complexes (see Gabrielsen *et al.* 1990) and formed through multiple events of extension since the collapse of the Caledonian orogen (e.g. Faleide *et al.* 1984, 1993, 2008; Gabrielsen *et al.* 1990; Gudlaugsson *et al.* 1998; Mosar *et al.* 2002; Glørstad-Clark *et al.* 2010). Post-Caledonian (Devonian) orogenic collapse was followed by several rift events throughout the Carboniferous to Eocene, terminating with the opening of the North Atlantic and Arctic oceans. The southwestern Barents Sea played an important role during the final stages of rifting, which was characterized by the transition from a simple rift system in the south to a dextral transform connecting the North Atlantic rift to the Arctic rift system in the NW (Faleide *et al.* 2008).

Despite the southwestern Barents Sea being subject to more than 300 myr of extension, several researchers have reported late Palaeozoic–Cenozoic events of tectonic inversion in the region (Ziegler 1978; Rønnevik *et al.* 1982; Berglund *et al.* 1986; Riis *et al.* 1986; Sund *et al.* 1986; Brekke & Riis 1987; Gabrielsen & Færseth 1989; Wood *et al.* 1989; Gabrielsen *et al.* 1990, 1997, 2011; Vågnes *et al.* 1998; Grogan *et al.* 1999; Glørstad-Clark *et al.* 2011; Henriksen *et al.* 2011; Faleide *et al.* 2015). The most prominent examples of this are found around the Loppa High (Fig. 1), where uplift of a late Triassic–mid-Jurassic depocentre in the early Cretaceous caused the high to form an island (Wood *et al.* 1989; Gabrielsen *et al.* 1990; Faleide *et al.* 1993*a*; Glørstad-Clark *et al.* 2011). The uplift was contemporaneous with transpression along the Bjørnøyrenna Fault Complex (Gabrielsen *et al.* 1997) and wrench-related tectonic inversion in the region (Rønnevik *et al.* 1982; Gabrielsen 1984; Berglund *et al.* 1986; Riis *et al.* 1986; Sund *et al.* 1986; Brekke & Riis 1987; Gabrielsen & Færseth 1988). Tectonic inversion also occurred in the region in the late Cretaceous–Paleocene owing to head-on (fault-perpendicular) contraction along the Bjørnøyrenna Fault Complex (Gabrielsen *et al.* 1997) and along the margins of the Veslemøy High and the Senja Ridge (Fig. 1; Riis *et al.* 1986; Brekke & Riis 1987; Breivik *et al.* 1998). Other events of inversion include latest Paleocene–Eocene transpression along the transform Senja Shear Zone margin in the west (Grogan *et al.* 1999; Faleide *et al.* 2008, 2015) and a Miocene SE-directed contraction (present coordinates) that is probably related to ridge push affiliated with the development of the mid-ocean Knipovich Ridge in the NW (Gabrielsen & Færseth 1989; Pascal *et al.* 2005; Engen *et al.* 2008; Faleide *et al.* 2015; Gac *et al.* 2016).

This paper focuses solely on the early Cretaceous phase of the tectonic inversion event. Although this phase of inversion has long been recognized, its exact timing and driving mechanism(s) are not yet fully constrained. We therefore describe the tectonic inversion structures that are associated with this event, and aim at constraining its timing and mechanism of initiation and development. The observations are set in a regional context and a tectonic model for the early Cretaceous tectonic development is presented.

Geological setting

Areas involved in the early Cretaceous phase of inversion include (1) the Loppa High and the Polhem Subplatform (2) the Hammerfest Basin and (3) the Bjørnøya and Tromsø basins (Fig. 1). Based on hitherto published information, these structural elements are described below.

The Loppa High is bordered by the Bjarmeland Platform in the east and is separated from the Polhem Subplatform to the west by the Jason Fault Complex (Fig. 1; Glørstad-Clark *et al.* 2011). The Polhem Subplatform, which was part of the greater Loppa High throughout much of its history, is bordered by the Ringvassøy–Loppa Fault Complex to its SW and the Bjørnøyrenna Fault Complex to its NW. The northeastern segment of the latter fault complex also defines the boundary between the Loppa High and the Bjørnøya Basin (Fig. 1).

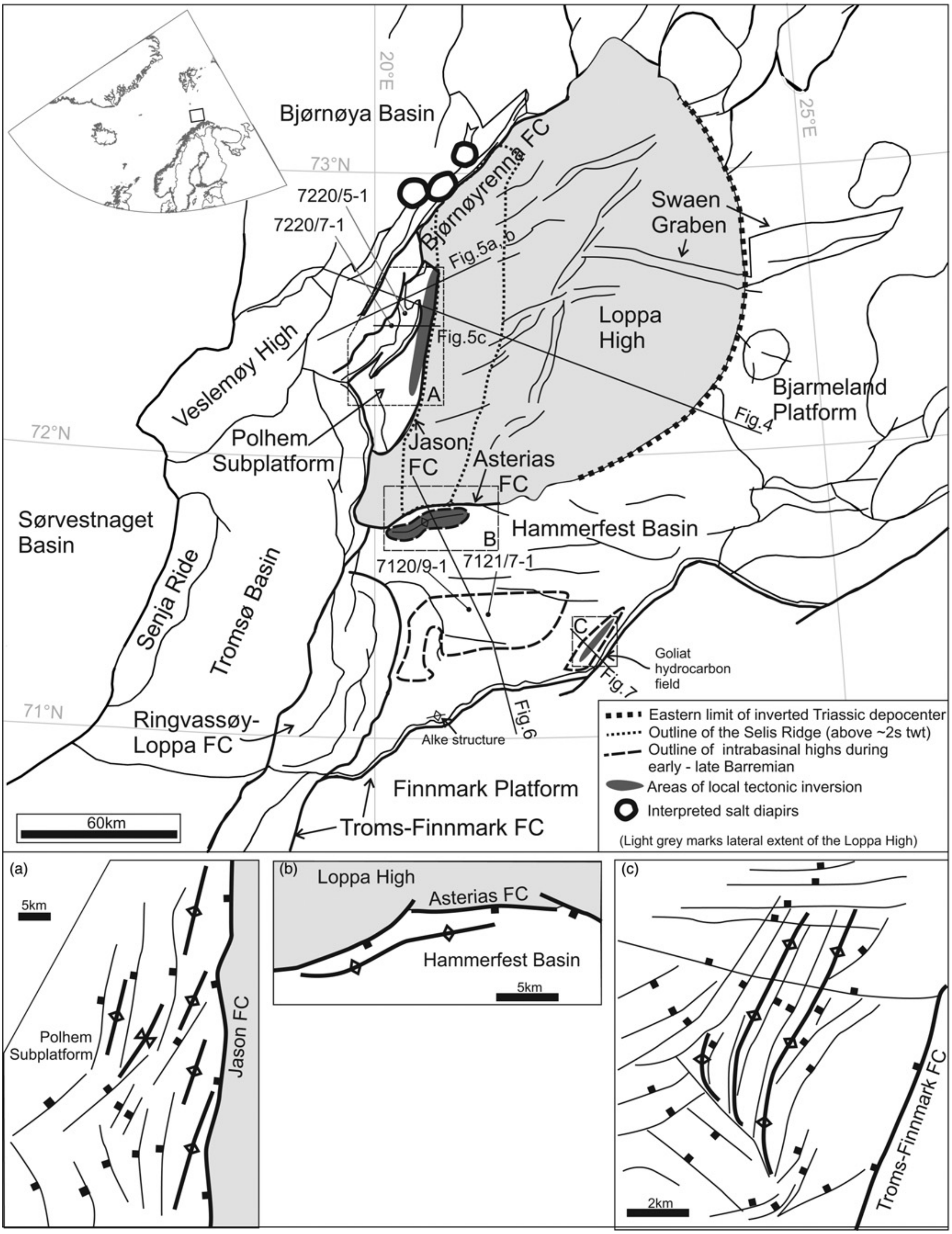

Fig. 1. Overview of the study area showing the main structural elements. The extent of the Loppa High is marked in light grey. Location of wells and key seismic lines used in the paper is given, in addition to the location of important structures discussed in the text (see legend for more details) (**a**) Detailed structural map of the Polhem Subplatform. (**b**) Detailed structural map of the Asterias Fault Complex and associated structures. (**c**) Detailed structural map of the Goliat hydrocarbon field area. Structural element map modified from Norwegian Petroleum Directorate (npd.no). FC, fault complex.

The Loppa High developed through several events of subsidence and uplift. Its predecessor, the Selis Ridge (also known as the ‘palaeo-Loppa High’; see Sund *et al.* 1986; Fig. 1) is now expressed as an easterly tilted high buried within the Loppa High. It formed by uplift of the footwall of the westerly dipping Ringvassøy–Loppa and Bjørnøyrenna fault complexes in late Carboniferous, early Permian, late Permian and early to middle Triassic (Riis *et al.* 1986; Wood *et al.* 1989; Gudlaugsson *et al.* 1998; Glørstad-Clark *et al.* 2010, 2011). The Polhem Subplatform formed as a downfaulted portion of the Selis Ridge in the early to mid-Triassic (Gabrielsen *et al.* 1990). By the mid-Triassic the Selis Ridge became expressed as a pronounced north–south-striking, elongated structural high acting as a barrier to sediments (Gudlaugsson *et al.* 1998; Glørstad-Clark *et al.* 2010). Subsequently, the Selis Ridge subsided and a major sediment depocentre was established atop the ridge by late Triassic times. In the late Jurassic or earliest Cretaceous, a wider platform around (and including) the Selis Ridge and Polhem Subplatform again became uplifted, causing the late Triassic–mid-Jurassic depocentre to form a subaerially exposed Loppa High (Fig. 1; Wood *et al.* 1989; Gabrielsen *et al.* 1990; Faleide *et al.* 1993*a*; Glørstad-Clark *et al.* 2011). The uplift is estimated to have been of the order of 300 m (see diagrams given by Clark *et al.* 2014). Erosion of the high and deposition of sediments along its flanks suggest gradual erosion and subsidence of the Loppa High in Q3 the early Cretaceous, bringing the Loppa High to the same level as the wider Barents Sea shelf by the onset of the Late Cretaceous (Glørstad-Clark *et al.* 2011).

The Hammerfest Basin is situated to the south of the Loppa High and is separated from the high by the southerly dipping Asterias Fault Complex (Fig. 1). This basin is delimited by the Ringvassøy–Loppa Fault Complex in the west, marking the down-stepping array of normal faults to the deeper Tromsø Basin further west (Gabrielsen 1984). To the east, the Hammerfest Basin gradually shallows and flexes to become the Bjarmeland Platform, and its southern boundary is defined by the north- to NW-dipping Troms–Finnmark Fault Complex (Gabrielsen *et al.* 1990).

The Hammerfest Basin was subject to extension throughout the Carboniferous–Eocene and its interior is characterized by a system of late Jurassic–early Cretaceous east–west-striking faults that have Q4 resulted in a range of minor horsts, grabens and half-grabens. On a larger scale, these define an east–west-striking arch that is oriented parallel to the basin axis. All these structures are most conveniently defined at the base of the Cretaceous sequence. The general basin configuration and the central arching of the basin axis have been ascribed to interaction between first-, second- and third-order normal faults (Gabrielsen 1984). Furthermore, it has been suggested that the deformational style indicates that the margins of the Hammerfest Basin were partly influenced by strike-slip reactivation in the late Jurassic to early Cretaceous (Berglund *et al.* 1986; Riis *et al.* 1986; Sund *et al.* 1986; Gabrielsen & Færseth 1988) as a part of regional wrench tectonics (Ziegler 1978; Rønnevik *et al.* 1982; Riis *et al.* 1986) probably caused by the oblique reactivation of pre-existing faults owing to changes in regional stress. This was assumed to result in inversion occurring along the western segment of the Asterias Fault Complex as fault-perpendicular contraction by Riis *et al.* (1986) and Gabrielsen & Færseth (1988). Alternatively, the inversion may have been affiliated with strike-slip forming a Hauterivian–Aptian positive half-flower-like structure as suggested by Gabrielsen *et al.* (2011). Transtension in the Swaen Graben as suggested by the presence of master faults steepening with depth, thus forming assumed positive and negative flower structures (Gabrielsen *et al.* 1993), occurred contemporaneously with inversion in the Hammerfest Basin and is therefore possibly genetically linked.

The Bjørnøya and Tromsø basins (Fig. 1) formed through rifting in the Carboniferous and Permian–early Triassic as is characterized by Permo-Carboniferous evaporite diapirs in both basins. Late Jurassic–earliest Cretaceous extension was followed by accelerating subsidence and accumulation of very thick sediment sequences of early Cretaceous age as demonstrated by the downfaulting of Jurassic sediments to *c.* 13 km depth in the Bjørnøya Basin across the Ringvassøy–Loppa and Bjørnøyrenna fault complexes (Rønnevik *et al.* 1982; Gabrielsen *et al.* 1990; Faleide *et al.* 1993*b*, 2008; Clark *et al.* 2014).

In summary, previous literature suggests an early Cretaceous period of composite tectonism in the southwestern Barents Sea, with distinct enhanced subsidence in the Tromsø and Bjørnøya basins, uplift of the Loppa High, and tectonic inversion that is probably related to regional wrenching.

Database

This study utilizes 2D reflection seismic data that are partly public data from the DISKOS database and partly non-public data made available by TGS and ENI Norge. Seismostratigraphic markers were picked using available public well data and are time-correlated in the Hammerfest Basin using biostratigraphic data from wells 7120/9-1 and 7121/7-1 and lithostratigraphy and chronostratigraphy from NORLEX (Figs 1 and 2; Worsley *et al.* 1988; Gradstein *et al.* 2010). On the Polhem Subplatform and in the Bjørnøya and Tromsø basins, the seismic markers were time-correlated using biostratigraphic data from wells 7220/5-1, 6-1 and 7-1 (Figs 1 and 2 and chronostratigraphy according to NORLEX). Depth conversion of regional grids has been done using the HiQbe™ velocity model (courtesy of First Geo AS and TGS-NOPEC Geophysical Company ASA) to obtain the geometry of the described structures.

Inversion structures

Several fault complexes and other structural elements in the southwestern Barents Sea display geometrical characteristics that are indicative of tectonic inversion. Some of these structures have previously been described in the literature, whereas others have not. Terminology and concepts used in this paper are given below and are followed by the description of early Cretaceous tectonic inversion structures in the southwestern Barents Sea and discussion of their genesis.

Terminology and concepts

Tectonic inversion is defined as the reverse reactivation of normal faults as a result of a change in the regional stress, resulting in uplift that predominantly affects the hanging wall relative to a selected regional reference stratigraphic level (Cooper *et al.* 1989). Tectonic inversion is commonly separated into localized (focused) and regional (distributed) inversion based on the significance of inversion within a rift (MacGregor 1995; see also Cooper & Williams 1989; Buchanan & Buchanan 1995). Whereas regional inversion commonly refers to the inversion of entire basins, localized inversion is often manifested as inversion structures with a local significance forming along reactivated normal faults.

A diagnostic criterion for recognizing and quantifying localized tectonic inversion is the identification of the ‘null point’ on inverted extensional faults (Fig. 3a; see Cooper & Williams 1989; Buchanan & Buchanan 1995; Turner & Williams 2004). The null point refers to a point along an inverted extensional fault that separates strata with normal fault displacement below and reverse fault displacement above. Because of the long rift history in the southwestern Barents Sea, however, the extension to shortening ratios seem too high for any null points to be detectable, rendering the use of the null-point criterion less relevant in the region. Alternative criteria for identifying reverse reactivation of normal faults are therefore

Colour online/mono hardcopy

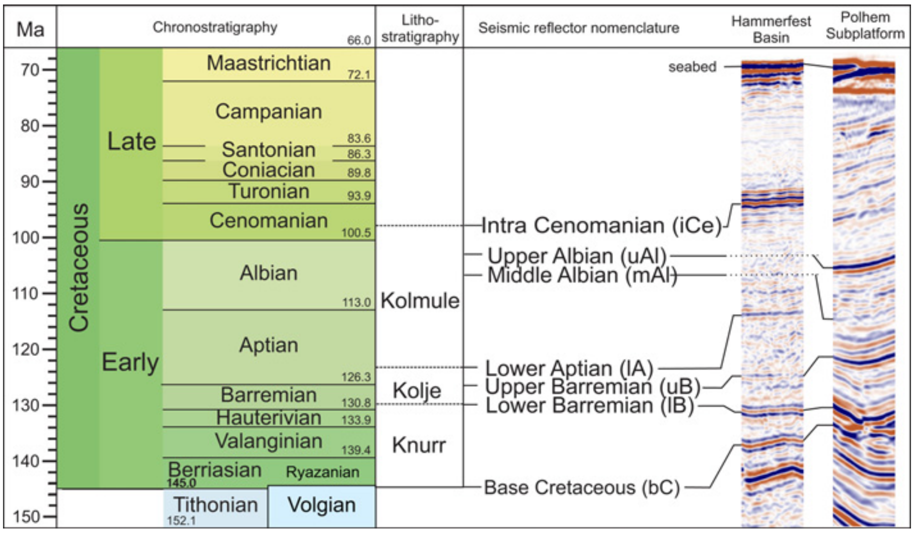

Fig. 2. Stratigraphic framework for the Hammerfest Basin and the Polhem Subplatform used in this paper. It should be noted that the lithostratigraphy is valid only for the Hammerfest Basin. Lithostratigraphy and chronostratigraphy from NORLEX (Worsley *et al.* 1988; Gradstein *et al.* 2010).

needed and include recognition of the following features: (1) inverted depocentre–growth wedges (without formation of null points); (2) contracted fault blocks and deformed fault planes; (3) forced folds with or without the development of hanging-wall reverse faults; (4) structures related to secondary contractional deformation of rift basins including the formation of folds and 'snake-head structures' (Allmendinger 1998) formed by reverse reactivation of faults (Fig. 3a–d). The timing of tectonic inversion is constrained by identifying pre-, syn- and post-rift sediments and their association with syn- and post-inversion sedimentary sequences (Fig. 3a; see also Turner & Williams 2004).

The Loppa High

The interior of the Loppa High constitutes an asymmetric high of sub-Carboniferous rocks that shallows westwards to include the Selis Ridge (Figs 1 and 4; see also Wood *et al.* 1989; Glørstad-Clark *et al.* 2011). The Selis Ridge formed during the Carboniferous and Permian events of uplift and defines a north–south-trending palaeo-high so that its eastern flank is onlapped by Carboniferous and Permian sedimentary units. The ridge is unconformly overlain by upper Triassic–mid-Jurassic sedimentary sequences that were uplifted during the early Cretaceous to form the Loppa High. These sequences show a distinct thickening from the Bjarmeland Platform and westward onto the present-day Loppa High (Fig. 4), where the zone of thickening of these units is characterized by a concentric shape in map view and also marks the eastern boundary of the inverted late Triassic–mid-Jurassic depocentre (Fig. 1). The concentric shape of the zone of thickening indicates that the lateral extent of the depocentre that controlled the extent of what later became uplifted, although the eastern boundary locally seems to be related to a fault present in the deeper strata (Fig. 4). Q5

The Jurassic and younger sedimentary sequences are in general missing on top of the Loppa High owing to erosion. However, lower Cretaceous sediments are locally present in a system of interacting NNE–SSW- and NE–SW-oriented *c.* 5 km wide grabens defined by the downfaulted upper Jurassic sequence (Figs 1 and 4). The system of grabens links up with the Swaen Graben in the east. The graben-bounding faults converge at depth and die out in Permian evaporites (Fig. 4).

Genesis.

The present-day Loppa High represents a regionally uplifted Triassic–Jurassic depocentre, as demonstrated by the distinct thickening of the upper Triassic–mid-Jurassic sediment sequence

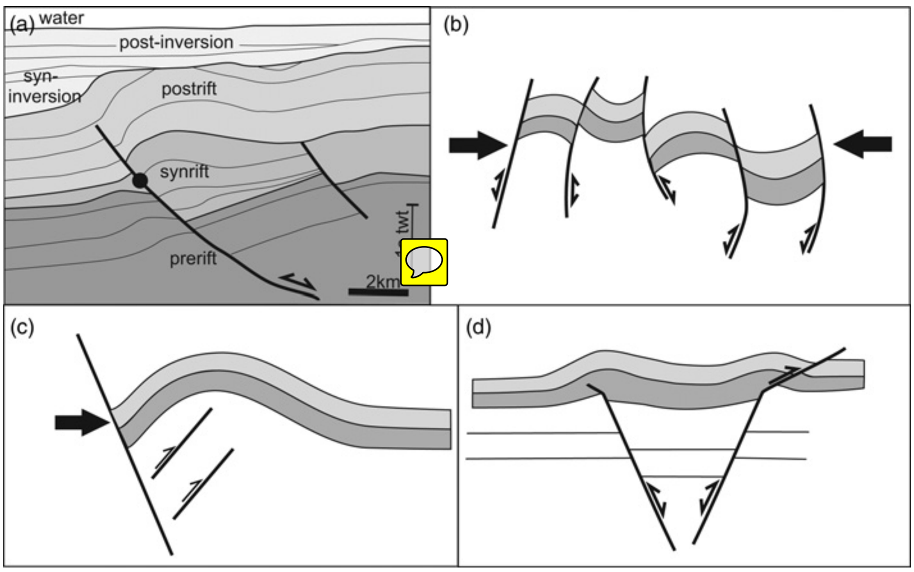

Fig. 3. Schematic overview of criteria used for identification of tectonic inversion in this paper. (**a**) Typical inversion geometry in an inverted half-graben showing the relationship between rift-related strata being modified by inversion. Black dot shows the position of the null point, which marks the divide between normal displacement below and reverse displacement above. Modified after Turner & Williams (2004). (**b**) Sketch of characteristic shapes of deformed fault blocks and deformed fault planes owing to horizontal shortening. (**c**) Folding through buckling owing to the localizing of inversion along a pre-existing normal fault. Reverse faults may or may not develop in the sub-strata. (**d**) Development of contractional structures such as snake-head folds and footwall cut-offs in synrift or post-rift sediments owing to reverse reactivation along an underlying normal fault.

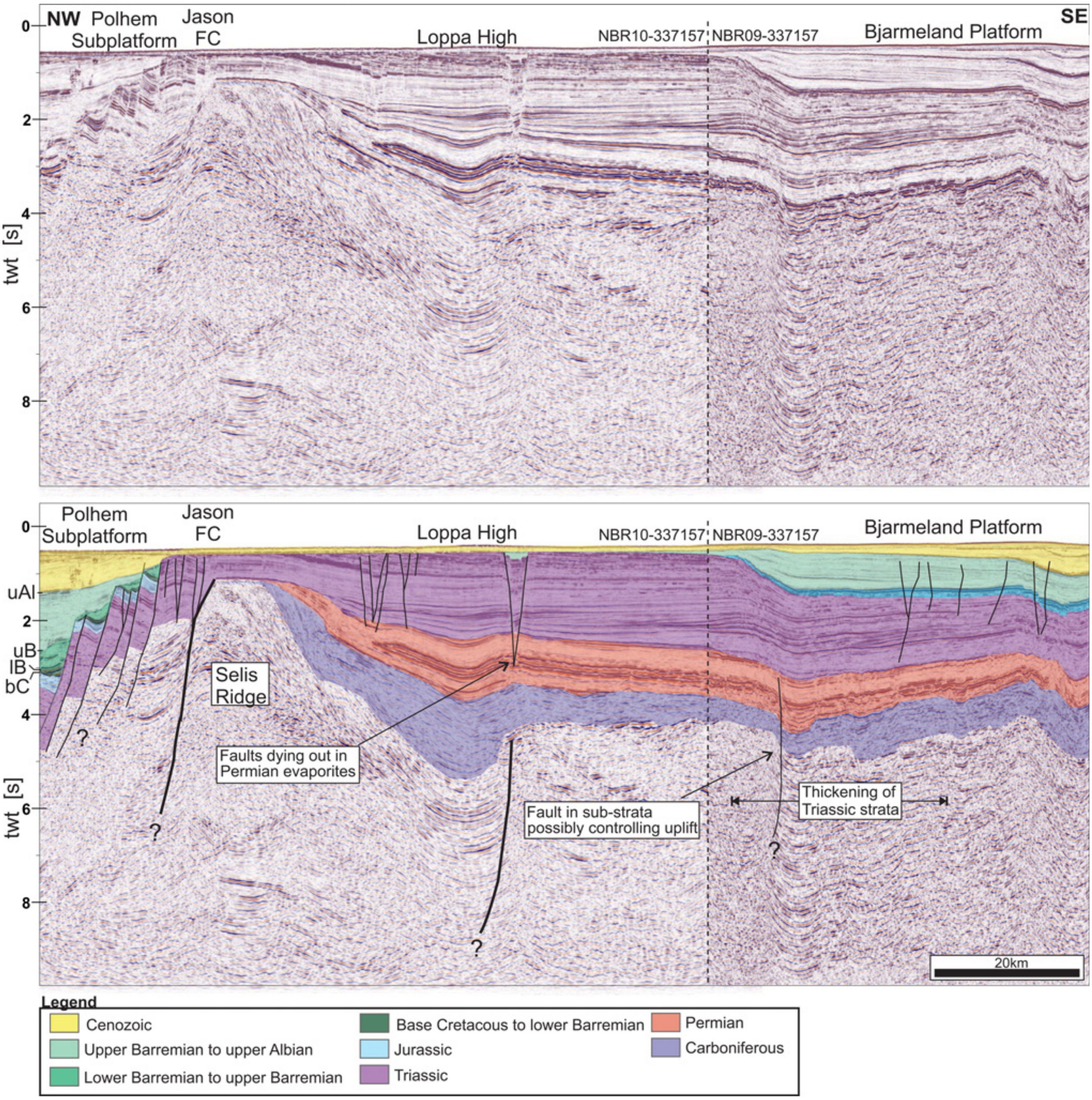

Fig. 4. Uninterpreted and interpreted seismic line running from the Bjarmeland Platform in the SE, across the Loppa High, Jason Fault Complex and the Polhem Subplatform in the NW. Names of seismic reflections are given along the left margin of the figure. (See Fig. 1 for location.)

Colour online/colour hardcopy

from the Bjarmeland Platform and westward onto the high (Fig. 4; see also Wood *et al*. 1989; Glørstad-Clark *et al*. 2011). Detailed mapping shows that the Swaen Graben links up with the narrow grabens within the interior of the Loppa High (Fig. 1) and they thus seem to be genetically linked. The role of these basins during early Cretaceous tectonic inversion will be further discussed when presenting a tectonic model later in the text.

The Polhem Subplatform

The Polhem Subplatform is composed of several north–south-striking rotated fault blocks, which are delineated by an array of down-to-the-west normal faults that are most easily identified at the base Cretaceous stratigraphic level (Fig. 5). Sedimentary wedges in the hanging walls indicate that the synsedimentary stage of faulting began in the late Jurassic and that subsidence accelerated from the early Barremian onwards. The sedimentary units that are located in the immediate vicinity of the Jason Fault Complex are characterized by the development of a series of densely spaced fault blocks comprising at least four anticlines arranged in a left-stepping, en echelon pattern with their fold axes at an angle of *c*. 15° clockwise to the Jason Fault Complex master fault (Fig. 1a). Seen in cross-section, the folds show the characteristics of positive flower structures (Fig. 5a–c). Together they make up a north–south-striking structural high that can be traced for *c*. 40 km within the hanging wall of the northern segment of the Jason Fault Complex (Fig. 1a). The crests of the anticlines are locally truncated by a pronounced erosional surface (Fig. 5b). Fault blocks located further west on the Polhem Subplatform are also commonly internally folded, however, so that strata dominantly dip steeply to the east (Fig. 5a and b). Local growth wedges of Ryazanian–late Barremian age within rotated fault blocks locally display evidence for localized inversion by reverse reactivation of graben-bounding faults and/or internal folding (Fig. 5c). The outer crests of the contracted fault

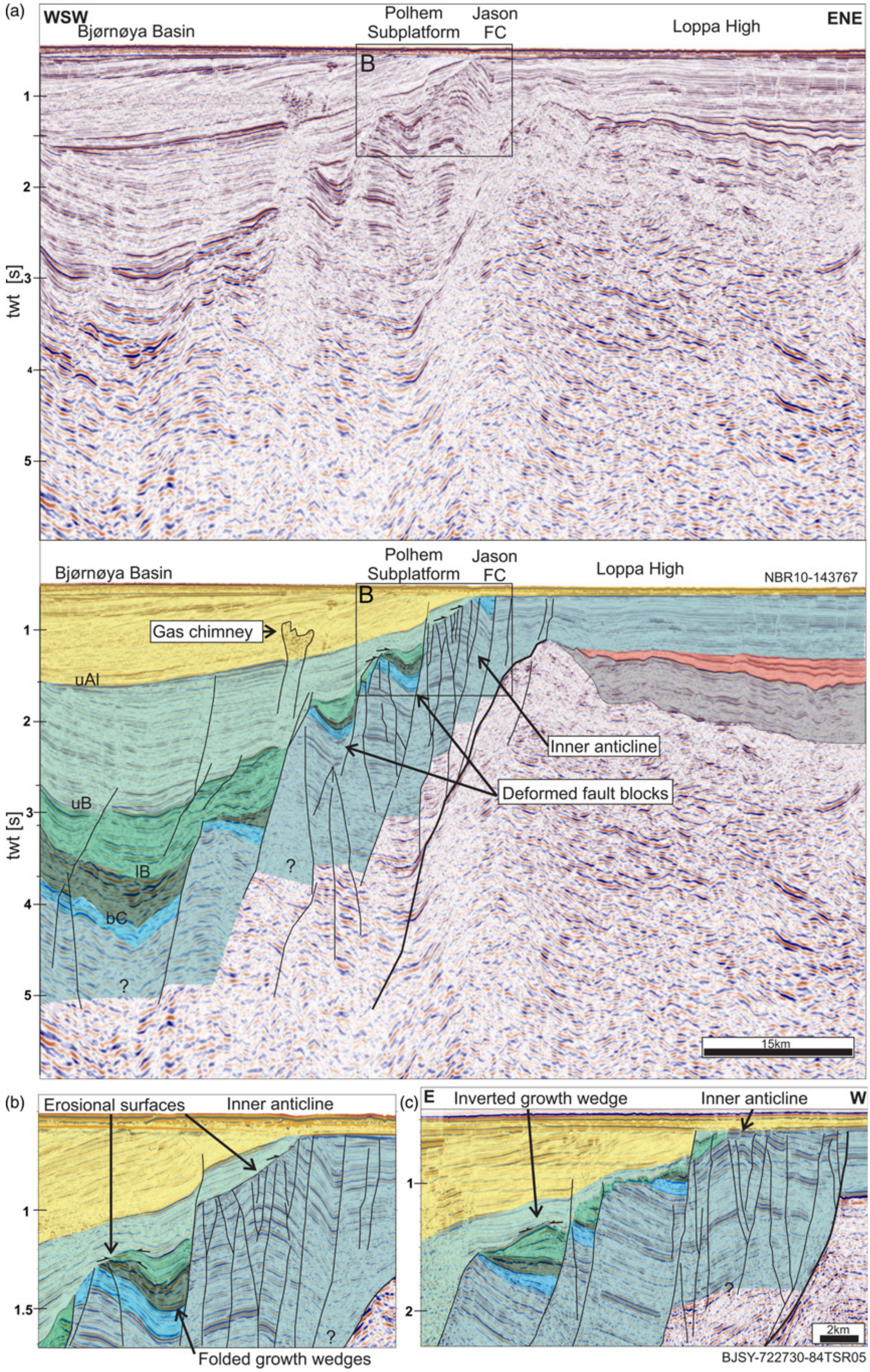

Fig. 5. (**a**) Uninterpreted and interpreted seismic line running across the Loppa High, Jason Fault Complex, Polhem Subplatform and into the Bjørnøya Basin. (**b**, **c**) Details from the same area. Small arrows indicate onlap. (See Fig. 1 for location.) Colour scheme as in Figure 4.

Colour online/ colour hardcopy

Q21

blocks are locally eroded and the erosional unconformity probably correlates in time with the erosional surface that truncates the inner, en echelon anticlines and demonstrates that contractional deformation predated or was contemporaneous with the erosion event. The upper Barremian sequence within the growth wedges onlaps the folded lower Barremian sequence (Fig. 5b). The upper Barremian unit is characterized by later minor modification by continued folding and is onlapped by the upper Barremian–middle Albian sedimentary sequence. Based on the onlap geometry within the inverted growth wedges, the timing of inversion on the Polhem Subplatform is constrained to the time interval between early Barremian and middle Albian.

Genesis.

The left-stepping, en echelon anticlines of the Polhem Subplatform with their fold axes oriented at *c.* 15° clockwise to the Jason Fault Complex indicate that the folds formed mainly as a result of east–west-oriented head-on contraction modified by sinistral shear in early Barremian to middle Albian time. This is in accordance with the internal characteristics of the inner anticlines that locally resemble positive flower structures (Fig. 5). The deformed fault blocks, faults and inverted growth wedges (Figs 1 and 5) most probably formed by the same contraction event, which caused internal buckle-folding and inversion of normal faults as illustrated in Figure 3b.

Gabrielsen *et al.* (1997) also suggested an early Cretaceous phase of transpression along the Bjørnøyrenna Fault Complex. They, however, suggested a dextral sense of shear for this event, but stated that determination of fold geometry and fold orientation was constrained by wide spacing of available seismic lines.

Notably, evidence for early Cretaceous inversion is not observed along the northern segment of the Bjørnøyrenna Fault Complex. The northern part of the Bjørnøyrenna Fault Complex was, however, affected by late Cretaceous–Paleocene head-on contraction (Gabrielsen *et al.* 1997). Present data also document the presence of salt diapirism in this area (Fig. 1). Analysis of the late Cretaceous–Paleocene inversion and salt diapirism are, however, beyond the scope of this paper and will not be addressed below.

The Hammerfest Basin

Several structures within and along some the marginal segments of the Hammerfest Basin display possible inversion structures.

Anticline parallel to the Asterias Fault Complex.

The Asterias Fault Complex partly detaches at the level of Permian evaporites (Fig. 6). The detachment is affected by north-dipping internal reflections offsetting the top of the Jurassic sequence, here interpreted as reverse faults (Fig. 6). A distinct east–west-striking anticline is located within its hanging wall (Fig. 1b). The anticline is best defined at the base of the Cretaceous level (Fig. 6) and its axis can be followed for *c.* 27 km, striking parallel to master faults of the fault complex. Its full wavelength, as measured between syncline minima bounding its flanks, is *c.* 8.3 km and its amplitude, as measured from a non-horizontal baseline connecting the syncline minima bounding its flanks, is *c.* 0.9 km.

The lower Barremian seismic marker represents the uppermost stratigraphic level that is influenced by the anticline. It is onlapped by an upper Barremian sequence. This sequence was modified by continued reverse fault activity (Fig. 6) and is onlapped by upper Barremian–lower Aptian sediments, which show no evidence for later structuring related to the anticline. The onlap relationships thus indicate that the anticline developed its major relief from early Barremian to early Aptian.

Genesis.

Based on the presence of reverse faults in its interior, the anticline within the hanging wall of the Asterias Fault Complex was most probably formed by north–south-directed contraction, overprinting earlier normal faults as a part of localized inversion. Horizontal shortening and the development of reverse faults led to the formation of the anticline as illustrated in Figure 3c. This is in accordance with interpretations of Riis *et al.* (1986) and Gabrielsen & Færseth (1988). Although it is difficult to exclude the possibility that inversion was the result of strike-slip movements along the Asterias Fault Complex as suggested by Gabrielsen *et al.* (2011), we conclude that the structure may satisfactorily be explained by head-on contraction alone.

Anticline associated with the Goliat hydrocarbon field.

This anticline encompasses the Goliat hydrocarbon field, which is located close to the intersection between east–west- and NE–SW-striking major segments of the Troms–Finnmark Fault Complex in the southeastern part of the Hammerfest Basin (Fig. 1; Mulrooney *et al.* in preparation). The anticline is most obvious at the base Cretaceous and deeper levels (Figs 1 and 7). Its axis can be traced for *c.* 30 km along-strike, within the hanging wall of the NE–SW-striking segment of the Troms–Finnmark Fault Complex (Fig. 1). Its full wavelength, as measured between syncline minima bounding its flanks, is *c.* 16 km and its amplitude, as measured from a baseline connecting the syncline minima bounding its flanks, is *c.* 0.9 km. It is onlapped by lower Barremian to lower Aptian strata in the NW, indicating that the anticline acted as an intrabasinal marginal high during that time. The crest of the anticline is characterized by minor faults that truncate the base Cretaceous reflection and show evidence for reverse reactivation as they terminate upwards within the cores of minor anticlines in above-lying Ryazanian–lower Barremian sediments (Fig. 7). The axes of the minor anticlines can be traced NE–SW, paralleling the strike of underlying faults for several kilometres. The minor anticlines accordingly strike parallel to the axis of the major anticline. Their wavelengths, as measured between the syncline minima bounding their flanks, are on average *c.* 0.5 km with an amplitude of *c.* 50 m, as measured from a baseline connecting the syncline minima. They are onlapped by lower Aptian sediments. Accordingly, the age of both the major anticline and the minor folds at its crest is constrained to the early Barremian to early Aptian.

Genesis.

The major anticline (Fig. 7) is probably the result of extension through the interaction of fault segments forming a fault-bound basement terrace with depth (Mulrooney *et al.* in preparation). It may thus be explained as an extensional feature. The minor folds affecting the lower Barremian reflection (Fig. 7), however, are interpreted to have formed owing to secondary contractional deformation and development of mild snake-head geometries caused by partial reverse reactivation of underlying faults as illustrated in Figure 3d. Locally, minor footwall cut-offs have developed owing to horizontal contraction (Fig. 7, inset). The amount of reverse reactivation is minor and consistent with NW–SE-oriented contraction causing localized inversion.

Farther west along the Troms–Finnmark Fault Complex, the Alke structure (Fig. 1; see also fig. 9 of Stewart *et al.* (1995) for profile) provides an additional example of possible tectonic inversion of similar age in the Hammerfest Basin. The Alke structure is affected by a local ramp–flat–ramp geometry of the Troms–Finnmark Fault Complex, but we suggest that the pronounced geometry of the structure indicates later contractional modification.

Central arch of the Hammerfest Basin.

A central arch strikes east–west within the interior of the Hammerfest Basin, parallel to the basin axis (Figs 1 and 6;

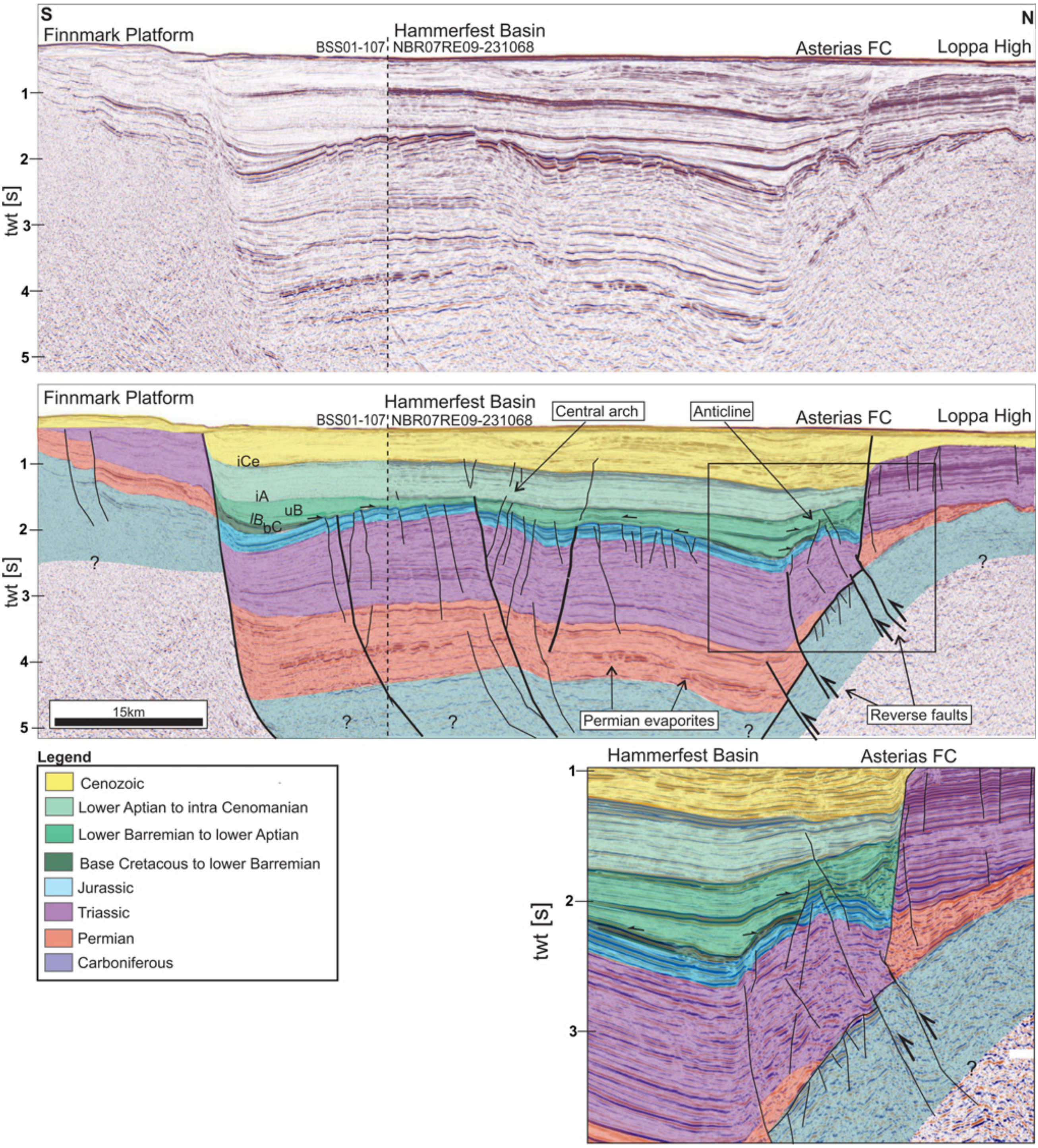

Fig. 6. Uninterpreted and interpreted seismic line running across the Hammerfest Basin, from Loppa High in the north to the Finnmark Platform in the south, crossing the Asterias and Troms–Finnmark fault complexes. Small arrows indicate onlap. (See Fig. 1 for location.)

Gabrielsen 1984; Berglund *et al.* 1986). It is most clearly observed at the base of the Cretaceous sequence and the arch axis can be followed for *c.* 80 km. The arch has a wavelength of *c.* 65 km, as measured between syncline minima bounding its flanks, and has an amplitude of *c.* 2.2 km (measured from a non-horizontal baseline connecting the syncline minima bounding its flanks). The arch is abruptly truncated by the Ringvassøy–Loppa Fault Complex in the west and gradually flattens towards the east. Internally, the arch is truncated by a north-dipping fault array with a combined displacement of *c.* 1 km (Fig. 6). The fault array divides the Hammerfest Basin into a southern and northern segment that together constitute two, partly rotated, large-scale fault blocks of opposite vergence (Fig. 6). The hinge line of the central arch coincides with the upward-rotated northern rim of the southern fault block, thus defining the main body of the central arch. The arch is onlapped by Ryazanian–upper Barremian seismic sequences from both north and south, demonstrating that the central arch (and thus the basin axis) acted as a structural high during the Ryazanian–late Barremian.

Genesis.

The central arch was an intrabasinal, southerly tilted high during the Ryazanian–Hauterivian to late Barremian as illustrated by its onlap configurations. The genesis of the central arch has previously been discussed in the literature, and has been ascribed either to the

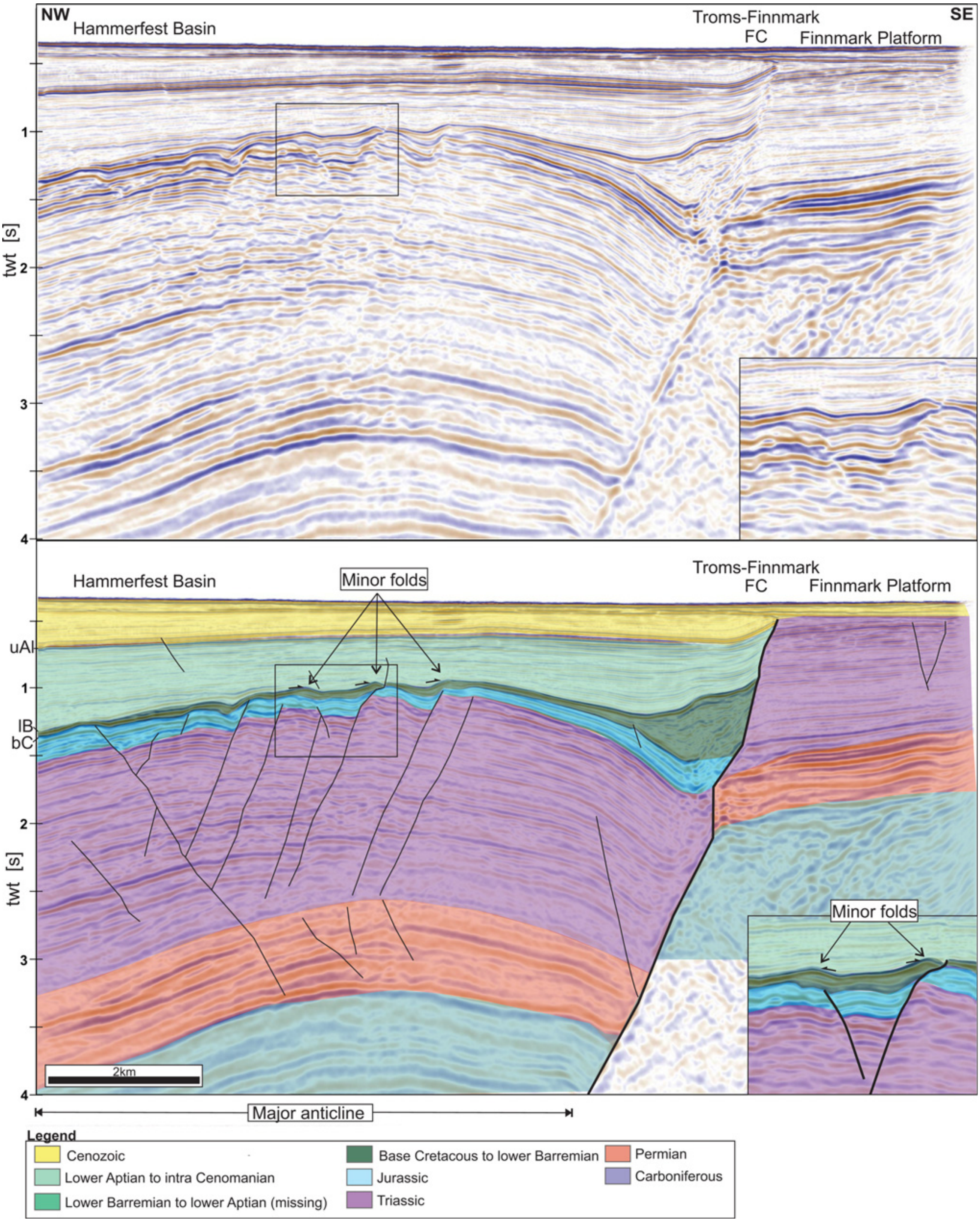

Colour online/colour hardcopy

Fig. 7. Uninterpreted and interpreted seismic line showing the major anticline associated with the Goliat hydrocarbon field. The minor folds on the crest of the anticline and the onlap geometry (inset) should be noted. Small arrows indicate onlap. Names of seismic reflections are given along the left margin of the figure (see Fig. 3). (See Fig. 1 for location.) Q22

interaction between first-, second- and third-order normal listric faults (Gabrielsen 1984), or to north–south-oriented shortening owing to strike-slip movements along the east–west-striking internal faults of the Hammerfest Basin (Berglund *et al*. 1986; Sund *et al.* 1986). The new generation seismic data reveal that the apex of the central arch coincides with the outer rim of the large-scale southern rotated fault block of the Hammerfest Basin and may hence explain the central arch as a product of extension. Further, the formation of the arch in the Ryazanian–Hauterivian indicates that the arch formed as a response to extension in the Hammerfest Basin rather than early Barremian inversion. The above favours the interpretation of Gabrielsen (1984), suggesting that the arch is the result of the interaction between first-, second- and third-order normal faults. Thus, in the present work, the central arch is not considered to be caused by tectonic inversion, although it still remains open whether the arch was later modified by horizontal shortening related to the early Barremian–early Aptian inversion along the Asterias Fault Complex, in the Goliat hydrocarbon field area and potentially also the Alke structure.

In summary, the Polhem Subplatform itself, the structures along its western margin (the Jason Fault Complex), the Asterias Fault Complex and minor folds associated with the Goliat hydrocarbon field area show characteristics consistent with early Cretaceous localized tectonic inversion that focused along parts of pre-existing major normal faults. Inversion structures associated with the Polhem Subplatform show evidence of being modified by sinistral strike-slip (Figs 1a, 3b and 5), whereas inversion in the Hammerfest Basin is consistent with north–south- and NE–SW-oriented head-on contraction (Figs 1b, c, 3c, d, 6 and 7). The inversion structures are associated with marginal intrabasinal highs that were subject to erosion, no sedimentation or low sedimentation rates during formation and are constrained to the early Barremian–early Aptian or early Barremian–middle Albian. It is important to stress that the inversion structures are clearly subordinate in relation to the rift activity occurring contemporaneously.

Tectonic model

According to our dating, the tectonic inversion of the Polhem Subplatform and in the Hammerfest Basin occurred contemporaneously (Fig. 8) and therefore it is logical to ascribe these events to one single tectonic event that began in the early Barremian. The inversion is, however, restricted only to parts of major fault complexes and shows inversion structures of diverse orientation (ENE–WSW, NE–SW and north–south; Fig. 1). Previous studies have suggested mechanisms involving regional wrenching events (Ziegler 1978; Rønnevik *et al*. 1982; Riis *et al*. 1986; Gabrielsen & Færseth 1988) causing oblique reactivation and strike-slip movements along already existing faults in an effort to explain the varying nature of shortening. Accordingly, Gabrielsen & Færseth (1988) suggested that a slight clockwise rotation of the Hammerfest Basin could explain inversion along the Asterias Fault Complex and east in the Hammerfest Basin. The driving force(s) behind such wrenching or rotation, however, has not yet been analysed in full, but may be attributed to a regional stress field or alternatively to stress of local significance caused by local tectonic adjustments. The present work shows that the timing of inversion is closely linked to the uplift of the Loppa High and that areas subject to inversion are located close to the high. We therefore suggest that there is a close link between the early Cretaceous uplift of the Loppa High, wrenching and the formation of the above-described inversion structures. We propose that inversion was a direct response to the uplift of the Loppa High and present the following model for the early Cretaceous tectonic inversion in the southwestern Barents Sea (Fig. 9).

The uplift of the Loppa High relative to its surroundings was probably accommodated by normal slip along its delimiting fault complexes; that is, the Bjørnøyrenna, Ringvassøy–Loppa and Asterias fault complexes, which all dip basinward. The geometrical relationship dictates that such uplift would lead to space accommodation problems along the flanks of the high owing to its widening with depth, assuming that the high and flanking basins are laterally confined (Fig. 9a). Upward-directed movement of the high is thus likely to have been converted into horizontal compressive stress along the flanks of the high. Stress generated by this mechanism would form perpendicular to the flank being utilized for uplift (Fig. 9a). This model is fundamentally different from the development of a 'classic' horst, where the widening of the horst with depth is compensated for by extension. Because separate flanks with contrasting orientations were utilized during uplift of the Loppa High, several local stress configurations may have developed, each dominated by σ_1 oriented perpendicular to the uplifted flank. The amount of shortening induced as a result of uplift may depend on (but is not restricted to) (1) the amount of vertical uplift and the dip of the fault being utilized to accommodate uplift, (2) the ability of sediments involved to compact and (3) the amount of extension occurring contemporaneously along the same fault (compensating for the widening of the high with depth).

By assuming a constant volume and fixed flanking basins (negligible compaction and extension) along a 2D section running perpendicular to, and across a fault utilized to accommodate uplift, the ratio between uplift and horizontal shortening may be given by the shortening ratio, $s_r = 1/\tan(\alpha)$, where α is the dip of fault on which uplift is accommodated (Fig. 9a and b). As no compaction of sediments and a 100% effective lateral confinement are highly unlikely assumptions, the shortening ratio must be considered a maximum estimate of shortening being generated by the discussed mechanism.

The geometrical relationship between the Asterias Fault Complex and the associated anticline caused by inversion (Fig. 6) can be used to test the applicability of the shortening ratio. The master fault segment of the western part of the Asterias Fault Complex dips 62° at the stratigraphic depth at which the anticline is located. The amount of horizontal shortening observed by the formation of the anticline (as measured between the syncline minima bounding the anticline) is calculated to be *c*. 1.2%, corresponding to *c*. 180 m. Using the shortening ratio (Fig. 9b), the amount of vertical uplift corresponding to the observed horizontal shortening is calculated to be *c*. 340 m. This value fits well with first-order estimates of the early Cretaceous uplift of the Loppa High of Clark *et al*. (2014, see diagrams within that paper), giving values of the order of 300 m.

Further, at least three mechanisms generating laterally varying stress configurations may exist. First, the Loppa High shows an asymmetric uplift along its east–west axis, increasing westwards (Fig. 4). Hence, the western flanks of the high may have been subject to greater amounts of fault throw and hence larger space accommodation problems than flanks along the eastern part of the high. As an example, inversion along only the western part of the east–west-striking Asterias Fault Complex supports this (Figs 1 and 6).

Second, variations in sediment compaction and/or amount of lateral confinement of flanking basins are likely and would significantly affect the amount of observable shortening being generated by uplift. This may be the reason why no inversion structures of early Cretaceous age are observed along the northern part of the Bjørnøyrenna Fault Complex, as extension and subsidence in this part of the Bjørnøya Basin may have been greater than shortening generated by uplift at the time.

Third, the asymmetric shape of the Loppa High would lead to an unbalanced local horizontal stress field being generated, assuming all flanks are utilized for uplift. In addition, shortening occurring within the Tromsø and Bjørnøya basins was probably less confined than in the Hammerfest Basin owing to continuing extension.

The model thus implies that stress generated by uplift varies in strength and orientation, leading to an unbalanced regional stress pattern. Rotation as a response to unbalanced local horizontal stress-fields being generated by uplift may thus be a source for a component of wrenching, as has been suggested in the region by several researchers (Ziegler 1978; Rønnevik *et al*. 1982; Berglund *et al*. 1986; Riis *et al*. 1986; Sund *et al*. 1986; Gabrielsen & Færseth 1988, 1989; Gabrielsen *et al*. 1997). In the case of the Loppa High, the resulting stress configuration could potentially have led to clockwise bulk rotation of the high around a vertical axis (Fig. 9c).

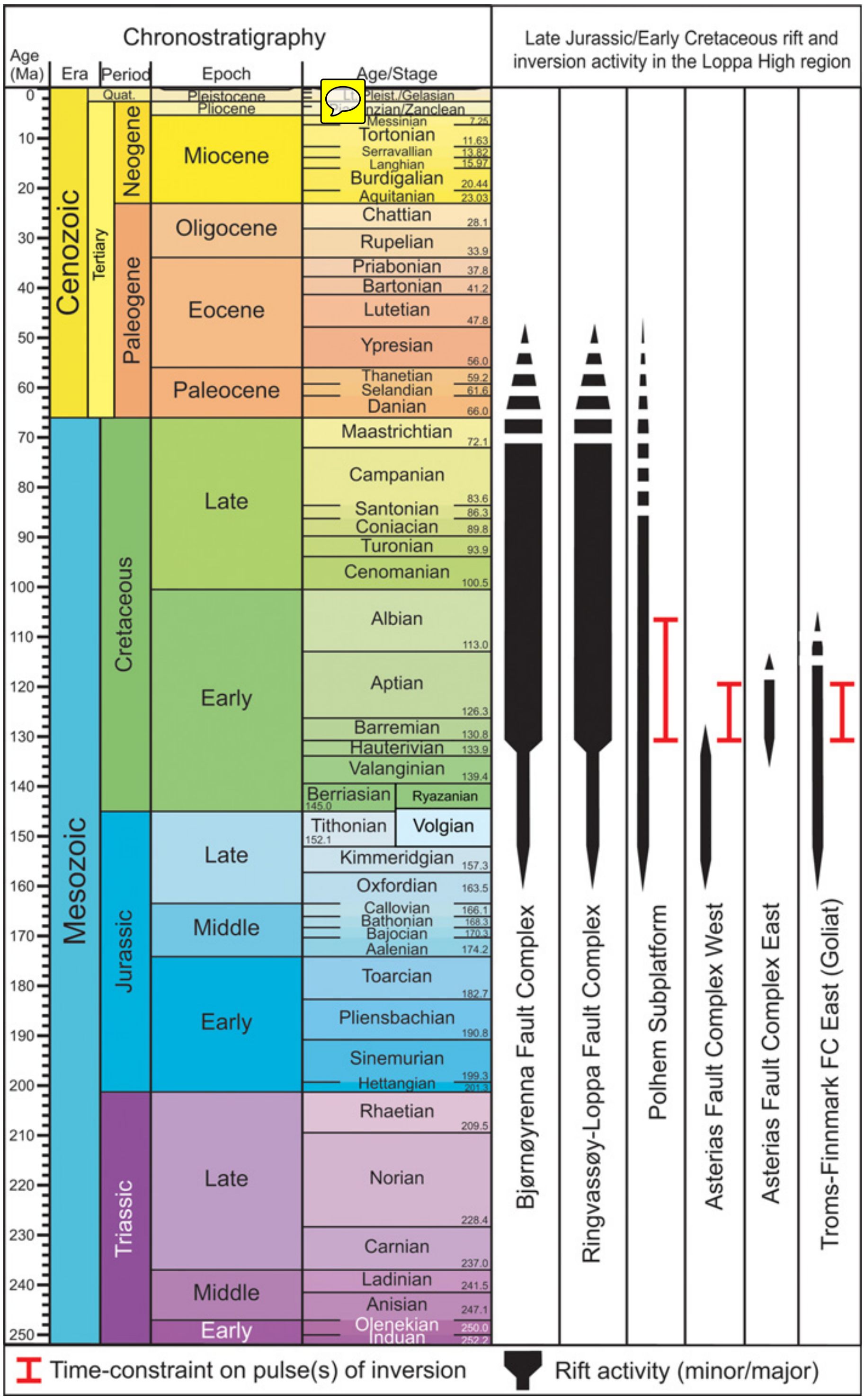

Fig. 8. Table summarizing Cretaceous rift activity in the region together with the constrained time interval for which the described tectonic inversion structures formed. Chronostratigraphy from Gradstein *et al*. (2010).

Such rotation would explain both sinistral movements on the Polhem Subplatform generating the observed en echelon folds and also transtension in the Swaen Graben and the associated narrow grabens in the interior of the Loppa High (Fig. 9c). However, it is not unlikely that far-field horizontal stresses contributed to strike-slip movements along the margins of the Loppa High in the early Cretaceous.

The inversion close to the Goliat hydrocarbon field (and potentially the Alke structure and partially the central arch of the Hammerfest Basin) is probably affiliated with horizontal stresses propagating from the Loppa High margins through basement units of the Hammerfest Basin. Numerical modelling has shown that stress is unlikely to propagate through relatively soft sedimentary cover units, but may propagate through crystalline basement for hundreds of kilometres and be expressed as passive folding of the above-lying sedimentary cover along basement-seated fault zones and or areas of high basement relief (e.g. Pascal & Gabrielsen 2001; Pascal *et al*. 2005, 2006, 2010; Buiter & Torsvik 2007; Cloething & Burov 2011; Doré *et al*. 2008). However, it cannot be excluded that the inversion structures located along the Troms–Finnmark Fault Complex are the result of far-field horizontal stresses.

The model constrains the initiation of uplift of the Loppa High to the early Barremian. It is noted that the uplift coincided with a major switch in rift activity in the region, where moderate, distributed extension in the late Jurassic or earliest Cretaceous in the southwestern Barents Sea was followed by major extension along

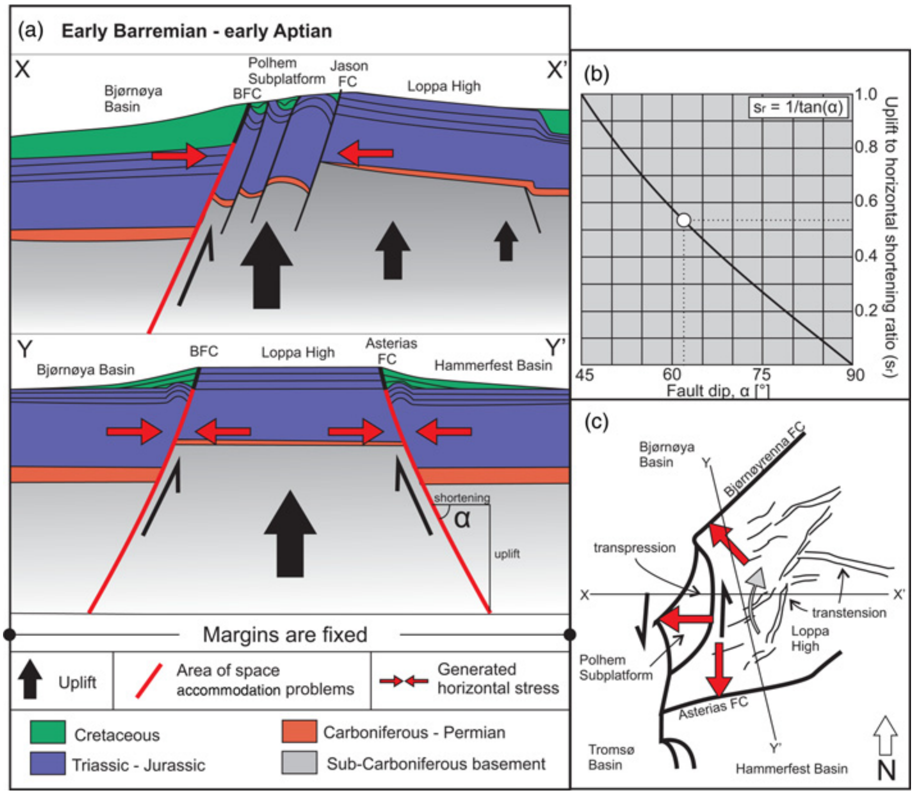

Colour online/colour hardcopy

Fig. 9. (**a**) Tectonic model showing how uplift of the Loppa High in the early Barremian to early Aptian may have been converted into horizontal stresses owing to space accommodation problems along its flanks. (See (**c**) for location and orientation of profiles.) (**b**) Graph showing the expected horizontal shortening to uplift ratio as a function of fault dip. White dot represents values for the Asterias Fault Complex. (**c**) Schematic illustration of horizontal stress generated by uplift (black arrows) and resulting horizontal clockwise rotation (grey arrow) owing to unbalanced horizontal stresses (red arrows) of the Loppa High. BFC, Bjørnøyrenna Fault Complex.

the Bjørnøyrenna and Ringvassøy–Loppa fault complexes by the early Barremian (Fig. 8; e.g. Gabrielsen *et al.* 1990; Faleide *et al.* 1993*a*,*b*, 2008). A focus of rift activity is recognized in the entire North Atlantic region and in the Barents Sea in this period (Faleide *et al.* 1993*b*), which in the southwestern Barents Sea led to extreme lithospheric thinning in the Tromsø and Bjørnøya basins. The axis defined by the Ringvassøy–Loppa and Bjørnøyrenna fault complexes marks the position of a major basement-seated Caledonian zone of weakness (Rønnevik *et al.* 1982; Gabrielsen *et al.* 1990; Faleide *et al.* 1993*a*,*b*, 2008; Ritzmann & Faleide 2007) and may explain why extension became focused in this zone.

The cause for uplift of the Loppa High has been previously discussed in the literature. Wood *et al.* (1989) suggested that uplift was associated with fault block rotation and footwall uplift along the Ringvassøy–Loppa and Bjørnøyrenna fault complexes. Such a mechanism is, however, commonly associated with uplift wavelengths from 0.1 to 15 km (Roberts & Yielding 1991; Gabrielsen *et al.* 2005) and thus fails to explain the uplift of the wider Loppa High area (wavelength >90 km). Uplift as a part of rift flank uplift owing to isostatic flexure has also been proposed (Glørstad-Clark *et al.* 2011; Clark *et al.* 2014). Although we agree that isostatic flexure most probably was involved in the uplift of the Loppa High, such uplift would affect the entire eastern flank of the Tromsø and Bjørnøya basins and thus cannot fully explain the uplift of the Loppa High relative to, for example, the neighbouring Hammerfest Basin situated along the same rift flank.

We therefore conclude that one or more additional process(es) must have contributed to the uplift of the Loppa High. Such mechanisms could include far-field stresses but also uplift mechanisms related to the deeper structuring of the high and thermomechanical processes, including *P*–*T*-related mineral transitions. It is particularly noted that the high is underlain by a distinct block of thicker crust (Ebbing & Olesen 2010), which is characterized by anomalously high densities and magnetic susceptibilities at its base interpreted to represent the presence of mafic rocks (Ritzmann & Faleide 2007; Clark *et al.* 2014). An increase in heat flux owing to lithospheric thinning in the west may have triggered uplift through thermal heating and/or phase changes in the lower mafic crust. These are, however, aspects that need to be tested and will not be further discussed herein.

Conclusions

Evidence for early Cretaceous tectonic inversion is documented on the Polhem Subplatform and in the Hammerfest Basin, southwestern Barents Sea. The inversion structures show a range of orientations that are consistent with head-on (fault-perpendicular) contraction modified by sinistral transpression on the Polhem Subplatform and head-on contraction along the Asterias Fault Complex and in the Goliat hydrocarbon field area close to the Troms–Finnmark Fault Complex. The timing of formation of these structures is constrained to the early Barremian–early Aptian and early Barremian–middle Albian.

A tectonic model is presented that links the formation of the inversion structures to the uplift of the Loppa High owing to space accommodation problems along the flanks of the high during uplift. The model constrains the initiation of uplift of the Loppa High to the early Barremian and explains how differential uplift and/or changing along-fault boundary conditions may have led to unbalanced horizontal stresses leading to a clockwise bulk rotation of the high around a vertical axis (i.e. wrenching), causing transpression on the Polhem Subplatform and transtension in the Swaen Graben and the Loppa High interior.

The cause of uplift of the Loppa High is poorly constrained, but it was contemporaneous with extreme lithospheric thinning in the Tromsø and Bjørnøya basins in the west. We suggest that isostatic flexuring, thermal heating and/or phase changes at deeper crustal levels are processes that may have been involved in driving the uplift, although these are aspects that need to be further tested.

Acknowledgements and Funding

The present work is part of the ARCEx project (Research Centre for Arctic Petroleum Exploration), which is funded by the Research Council of Norway (grant number 228107) together with 10 academic and nine industry partners. We sincerely thank the reviewers A. Doré and R. Holdsworth for thorough and constructive feedback during the review process. We thank TGS-NOPEC Geophysical Company ASA and ENI Norge AS for access to seismic data, and TGS-NOPEC Geophysical Company ASA and First Geo AS for access to the HiQbe™ velocity model.

Scientific editing by Peter Clift

References

Allmendinger, R.W. 1998. Inverse and forward numerical modeling of trishear fault-propagation folds. *Tectonics*, **17**, 640–656.

Berglund, L.T., Augustson, J., Færseth, R., Gjelberg, J. & Ramberg-Moe, H. 1986. The evolution of the Hammerfest Basin. *In: Habitat of Hydrocarbons on the Norwegian Continental Shelf*. Graham & Trotman, London, 319–338. Q8

Breivik, A.J., Faleide, J.I. & Gudlaugsson, S.T. 1998. Southwestern Barents Sea margin: late Mesozoic sedimentary basins and crustal extension. *Tectonophysics*, **293**, 21–44.

Brekke, H. & Riis, F. 1987. Tectonics and basin evolution of the Norwegian shelf between 62°N and 72°N. *Norsk Geologisk Tidsskrift*, **67**, 295–322.

Buchanan, J.G. & Buchanan, P.G. (eds) 1995. *Basin Inversion*. Geological Society, London, Special Publications, **88**, http://doi.org/10.1144/GSL.SP.1995.088.01.30

Buiter, S.J.H. & Torsvik, T.H. 2007. Horizontal movements in the eastern Barents Sea constrained by numerical models and plate reconstructions. *Geophysical Journal International*, **171**, 1376–1389, http://doi.org/10.1111/j.1365-246X.2007.03595.x

Clark, S.A., Glorstad-Clark, E., Faleide, J.I., Schmid, D., Hartz, E.H. & Fjeldskaar, W. 2014. Southwest Barents Sea rift basin evolution: comparing results from backstripping and time-forward modelling. *Basin Research*, **26**, 550–566.

Cloething & Burov 2011 (details to be added by author).

Cooper, M.A. & Williams, G.D. (eds) 1989. *Inversion Tectonics*. Geological Society, London, Special Publications, **44**, http://doi.org/10.1144/GSL.SP.1989.044.01.25

Cooper, M.A., Williams, G.D. *et al.* 1989. Inversion tectonics—a discussion. *In*: Cooper, M.A. & Williams, G.D. (eds) *Inversion Tectonics*. Geological Society, London, Special Publications, **44**, 335–347, http://doi.org/10.1144/GSL.SP.1989.044.01.18

Doré, A.G. 1991. The structural foundation and evolution of Mesozoic seaways between Europe and the Arctic. *Palaeogeography, Palaeoclimatology, Palaeoecology*, **87**, 441–492. Q9

Doré, A.G., Lundin, E.R., Kusznir, N.J. & Pascal, C. 2008. Potential mechanisms for the genesis of Cenozoic domal structures on the NE Atlantic margin: pros, cons and some new ideas. *In*: Johnson, H., Doré, A.G., Gatliff, R.W., Holdsworth, R.W., Lundin, E.R. & Ritchie, J.D. (eds) *The Nature and Origin of Compression in Passive Margins*. Geological Society, London, Special Publications, **306**, 1–26, http://doi.org/10.1144/SP306.1

Ebbing, J. & Olesen, O. 2010. New compilation of top basement and basement thickness for the Norwegian continental shelf reveals the segmentation of the passive margin system. In: Vining, B.A. & Pickering, S.C. (eds) *Petroleum Geology: From Mature Basins to New Frontiers—Proceedings of the 7th Petroleum Geology Conference*. Geological Society, London, 885–897, http://doi.org/10.1144/0070885

Engen, Ø., Faleide, J.I. & Dyreng, T.K. 2008. Opening of the Fram Strait gateway: A review of plate tectonic constraints. *Tectonophysics*, **450**, 51–69.

Faleide, J.I., Gudlaugsson, S.T. & Jacquart, G. 1984. Evolution of the western Barents Sea. *Marine and Petroleum Geology*, **1**. Q10

Faleide, J.I., Vågnes, E. & Gudlaugsson, S.T. 1993*a*. Late Mesozoic–Cenozoic evolution of the southwestern Barents Sea. *In*: Parker, J.R. (ed.) *Petroleum Geology of Northwest Europe; Proceedings of the 4th Conference*. Geological Society, London, 933–950, http://doi.org/10.1144/0040933

Faleide, J.I., Vågnes, E. & Gudlaugsson, S.T. 1993*b*. Late Mesozoic–Cenozoic evolution of the south-western Barents Sea in a regional rift-shear tectonic setting. *Marine and Petroleum Geology*, **10**, 186–214.

Faleide, J.I., Tsikalas, F., Breivik, A.J., Mjelde, R., Ritzmann, O., Engen, O. & Eldholm, O. 2008. Structure and evolution of the continental margin off Norway and the Barents Sea. *Episodes*, **31**, 82–91.

Faleide, J.I., Gabrielsen, R.H., Indrevær, K., Gac, S., Faisal, M.F. & Pascal, C. 2015. Contractional events in the Barents Sea Basin evolution—timing, causes and implications. *In*: *Abstracts, 3P Arctic Conference, 29 September–2 October, 2015, Stavanger*. Q11

Gabrielsen, R.H. 1984. Long-lived fault zones and their influence on the tectonic development of the south-western Barents Sea. *Journal of the Geological Society, London*, **141**, 651–662, http://doi.org/10.1144/gsjgs.141.4.0651

Gabrielsen, R.H. & Færseth, R.B. 1988. Cretaceous and Tertiary reactivation of master fault zones of the Barents Sea. *In*: Dallmann, W.K., Ohta, Y. & Andresen, A. (eds) *Tertiary Tectonics of Svalbard. Extended Abstracts from Symposium Held in Oslo*. Norwegian Polar Institute Report Series, **46**, 93–97 [extended abstract].

Gabrielsen, R.H. & Færseth, R.B. 1989. The inner shelf of North Cape, Norway and its implications for the Barents Shelf–Finnmark Caledonide boundary. A comment. *Norsk Geologisk Tidsskrift*, **69**, 57–62.

Gabrielsen, R.H., Faerseth, R.B. & Jensen, L.N. 1990. *Structural Elements of the Norwegian Continental Shelf, Part. 1. The Barents Sea Region*. Norwegian Petroleum Directorate, Stavanger.

Gabrielsen, R.H., Grunnaleite, I. & Ottesen, S. 1993. Reactivation of fault complexes in the Loppa High area, southwestern Barents Sea. *In*: *Arctic Geology and Petroleum Potential*, **2**. Elsevier, Amsterdam, 631–641. Q12

Gabrielsen, R.H., Grunnaleite, I. & Rasmussen, E. 1997. Cretaceous and Tertiary inversion in the Bjørnøyrenna Fault Complex, south-western Barents Sea. *Marine and Petroleum Geology*, **14**, 165–178.

Gabrielsen, R.H., Braathen, A., Olesen, O., Faleide, J.I., Kyrkjebø, R. & Redfield, T.F. 2005. Vertical movements in south-western Fennoscandia: a discussion of regions and processes from the Present to the Devonian. *In*: Norwegian Petroleum Society Special Publications, **12**, 1–28. Q13

Gabrielsen, R.H., Faleide, J.I., Leever, K.A. & Grunnaleite, I. 2011. *Strike-slip related inversion-tectonics of the southwestern Barents Sea (Norwegian Shelf) in a plate tectonic perspective*. EGU General Assembly 2011. *Geophysical Research Abstracts*, **13**. Q14

Gac, S., Klitzke, P., Minakov, A., Faleide, J.I. & Scheck-Wenderoth, M. 2016. Lithospheric strength and elastic thickness of the Barents Sea and Kara Sea region. *Tectonophysics*, http://doi.org/10.1016/j.tecto.2016.04.028.

Glørstad-Clark, E., Faleide, J.I., Lundschien, B.A. & Nystuen, J.P. 2010. Triassic seismic sequence stratigraphy and paleogeography of the western Barents Sea area. *Marine and Petroleum Geology*, **27**, 1448–1475.

Glørstad-Clark, E., Clark, S.A., Faleide, J.I., Bjørkesett, S.S., Gabrielsen, R.H. & Nystuen, J.P. 2011. Basin dynamics of the Loppa High area, SW Barents Sea: A history of complex vertical movements in an epicontinental basin. *In*: Glørstad-Clark, E. (ed.) *Basin analysis in western Barents Sea area: The interplay between accommodation space and depositional system*. PhD thesis, University of Oslo. Q15

Gradstein, F.M., Anthonissen, E., Brunstad, H., Charnock, M., Hammer, O. Hellem, T. & Lervik, K.S. 2010. Norwegian offshore stratigraphic lexicon (NORLEX). *Newsletters on Stratigraphy*, **44**, 73–86.

Grogan, P., Østvedt-Ghazi, A.M., Larssen, G.B., Fotland, B., Nyberg, K., Dahlgren, S. & Eidvin, T. 1999. Structural elements and petroleum geology of the Norwegian sector of the northern Barents Sea. *In*: Fleet, A.J. & Boldy, S.A. R. (eds) *Petroleum Geology of Northwest Europe: Proceedings of the 5th Conference*. Geological Society, London, 247–259, http://doi.org/10.1144/0050247

Gudlaugsson, S.T., Faleide, J.I., Johansen, S.E. & Breivik, A.J. 1998. Late Palaeozoic structural development of the south-western Barents Sea. *Marine and Petroleum Geology*, **15**, 73–102.

Henriksen, E., Ryseth, A.E., Larssen, G.B., Heide, T., Rønning, K., Sollid, K. & Stoupakova, A.V. 2011. Tectonostratigraphy of the greater Barents Sea: implications for petroleum systems. *In*: Spencer, A.M., Embry, A.F., Gautier, D.L., Stoupakova, A.V. & Sørensen, K. (eds) *Arctic Petroleum Geology*. Geological Society, London, Memoirs, **35**, 163–195, http://doi.org/10.1144/M35.10

Macgregor, D.S. 1995. Hydrocarbon habitat and classification of inverted rift basins. *In*: Buchanan, J.G. & Buchanan, P.G. (eds) *Basin Inversion*. Geological Society, London, Special Publications, **88**, 83–93, http://doi.org/10.1144/GSL.SP.1995.088.01.06

Mosar, J., Eide, E.A., Osmundsen, P.T., Sommaruga, A. & Torsvik, T.H. 2002. Greenland–Norway separation: a geodynamic model for the North Atlantic. *Norwegian Journal of Geology*, **82**, 282.

Pascal, C. & Gabrielsen, R.H. 2001. Numerical modelling of Cenozoic stress patterns in the mid Norwegian Margin and the northern North Sea. *Tectonics*, **20**, 585–599.

Pascal, C., Roberts, D. & Gabrielsen, R.H. 2005. Quantification of neotectonic stress orientations and magnitudes from field observations in Finnmark, northern Norway. *Journal of Structural Geology*, **27**, 859–870.

Pascal, C., Roberts, D. & Gabrielsen, R.H. 2006. Present-day stress orientations in Norway as deduced from stress-release features. *In*: Lu, M., Li, C.C., Kjørholt, H. & Dahle, H. (eds) *In-situ Rock Stress. Measurement, Interpretation and Application*. Taylor & Francis, London, 209–213.

Pascal, C., Roberts, D. & Gabrielsen, R.H. 2010. Tectonic significance of present-day stress relief phenomena in formerly glaciated regions. *Journal of the Geological Society, London*, **167**, 363–371, http://doi.org/10.1144/0016-76492009-136

Riis, F., Vollset, J. & Sand, M. 1986. Tectonic development of the western margin of the Barents Sea and adjacent areas. Q16

Ritzmann, O. & Faleide, J.I. 2007. Caledonian basement of the western Barents Sea. *Tectonics*, **26**. Q17

Roberts, A.M. & Yielding, G. 1991. Deformation around basin-margin faults in the North Sea/mid-Norway rift. *In*: Roberts, A.M., Yielding, G. & Freeman, B. (eds) *The Geometry of Normal Faults*. Geological Society, London, Special Publication, **56**, 61–78, http://doi.org/10.1144/GSL.SP.1991.056.01.05

Rønnevik, H., Beskow, B. & Jacobsen, H.P. 1982. Structural and stratigraphic evolution of the Barents Sea. *In*: *Arctic Geology and Geophysics: Proceedings of the Third International Symposium on Arctic Geology*. Canadian Society of Petroleum Geologists, Memoir, **8**, 431–440. Q18

Stewart, D.J., Berge, K. & Bowlin, B. 1995. Exploration trends in the southern Barents Sea. *In*: Norwegian Petroleum Society Special Publications, **4**, 253–276. Q19

Sund, T., Skarpnes, O., Jensen, L.N. & Larsen, R.M. 1986. Tectonic development and hydrocarbon potential offshore Troms, Northern Norway. *In*: Halbouty, N.T. (ed.) *Future Petroleum Provinces of the World*. AAPG Memoirs, **40**, 615–628.

Turner, J.P. & Williams, G.A. 2004. Sedimentary basin inversion and intra-plate shortening. *Earth-Science Reviews*, **65**, 277–304.

Vågnes, E., Gabrielsen, R.H. & Haremo, P. 1998. Late Cretaceous–Cenozoic intraplate contractional deformation at the Norwegian continental shelf: timing, magnitude and regional implications. *Tectonophysics*, **300**, 29–46.

Wood, R.J., Edrich, S.P. & Hutchison, I. 1989. Influence of North Atlantic tectonics on the large-scale uplift of the Stappen High and Loppa High, western Barents Shelf. *In*: *Extensional Tectonics and Stratigraphy of the North Atlantic Margins*. AAPG Memoirs, **46**, 559–566.

Worsley, D., Johansen, R. & Kristensen, S.E. 1988. The Mesozoic and Cenozoic succession of Tromsøflaket. A lithostratigraphic scheme for the Mesozoic and Cenozoic succession offshore mid- and northern Norway. *In*: Dalland, A., Worsley, D. & Ofstad, K. (eds) *A Lithostratigraphic Scheme for the Mesozoic and Cenozoic and Succession Offshore Mid- and Northern Norway*. Norwegian Petroleum Directorate Bulletin, **4**, 42–65.

Ziegler, P.A. 1978. North-western Europe: tectonics and basin development. *Geologie en Mijnbouw*, **57**, 589–626.